O.L. MASLYANCHUK,[1] T. AOKI,[2] V.M. SKLYARCHUK,[1] S.V. MELNYCHUK,[1] L.A. KOSYACHENKO,[1] E.V. GRUSHKO[1]

[1] Yu. Fed'kovich National University of Chernivtsi
(2, Kotsyubyns'kyi Str., Chernivtsi 58012, Ukraine; e-mail: emaslyanchuk@yahoo.com)
[2] Research Institute of Electronics, Shizuoka University
(Johoku, Hamamatsu 432-8011, Japan)

PACS 72.80.Ey, 78.70. Dm

HIGH-EFFICIENCY CADMIUM TELLURIDE DETECTORS OF X- AND γ-RADIATION

Electric parameters of chlorine-doped CdTe crystals with a resistivity of (3÷6)× × 10^9 Ω·cm have been studied. The heavily doped material was characterized by an almost intrinsic conductivity, which is explained on the basis of the charge-carrier statistics by an emergence of self-compensated complexes. The ionization energy and the compensation degree of the impurity responsible for the semiinsulating state of CdTe are determined. The reverse current-voltage characteristics of the Ni/CdTe/Ni structure with a Schottky diode are interpreted as those of X/γ-radiation detectors with extremely low values of "dark" currents of about 5 nA at a voltage of 1500 V and a Schottky contact area of 0.1 cm^2 (at 300 K*). Results testifying to a detector energy resolution of 0.42% for the spectrum of ^{137}Cs isotope at an applied voltage of 1200 V and a temperature of 300* K *have been reported. The dependence of the detection efficiency on the concentration of noncompensated impurities (defects) N, which determines the width of the space charge region in the diode, is proved to be described by a function with a maximum located at $N \approx 2 \times 10^{11}$ cm^{-3} for ^{137}Cs isotope. By comparing the spectra obtained while irradiating the detector from either the Schottky or ohmic contact side, the concentration of noncompensated impurities in the studied crystals (of about 10^{12} cm^{-3}) is determined, which is close to the optimum N value.*

Keywords: CdTe-based X- and γ-ray detectors, compensation of semiconductor conductivity, detector with a Schottky diode, charge collection efficiency, detection efficiency of a Schottky diode detector, width of the space charge region, concentration of uncompensated impurities, energy resolution.

1. Introduction

Cadmium telluride (CdTe) is a basic semiconducting material for the manufacture of high-efficiency detectors of X- and γ-radiation (below, X/γ-radiation). In contrast to their silicon and germanium analogs, they can operate without cryogenic cooling. The possibility of the use of CdTe in detectors with a $p-n$ transition or a surface-barrier structure for the registration and the spectroscopy of γ-quanta (as well as α- and β-particles) was demonstrated as early as in the middle of the 1960s [1, 2]. The space charge region (SCR) in those detectors and in detectors studied within next years did not exceed 50-100 μm even if the maximum voltage was applied to the detector, which restricted the energy of detected quanta by a value of about 100 keV from above. The mobility μ of charge carriers was rather high. Despite that, since the corresponding lifetime τ was short – so that the product $\mu\tau$, one of the key characteristics of the materials intended to be used in detectors, was small – the en-

ergy resolution was too low for practical applications of such detectors [1–3]. Therefore, the technologies aimed at growing homogeneous and defect-free CdTe crystals with a high resistivity ($\rho > 10^9$ $\Omega \times$ cm at 300 K) for their use in detectors with ohmic contacts, in which the electric field acts in the whole crystal rather than in a narrow SCR only, were continuously sought. A configuration of electrodes, for which the energy resolution is governed only by electrons with a much higher mobility than that of holes, was also designed.

At the beginning of the 1990s, an alloy on the basis of CdTe, namely $Cd_{1-x}Zn_xTe$, was proposed to be used in detectors of X/γ-quanta. It was considered that the homogeneity and the structural perfection of $Cd_{1-x}Zn_xTe$ crystals could be made much better in comparison with the corresponding CdTe parameters. In addition, the substitution of Cd atoms by Zn ones broadens the energy gap in the semiconductor and, as a result, gives rise to a substantial growth of the resistivity to $\rho > 10^{10} \div 10^{11}$ $\Omega \times$ cm at $x = 0.05 \div 0.2$ (at 300 K), which makes "dark" currents (leakage currents) lower at enhanced voltages. However, expectancies put on $Cd_{1-x}Zn_xTe$ have not been justified in full. The leading companies continued to manufacture detectors on the basis of both $Cd_{1-x}Zn_xTe$ and CdTe. The seeking of new materials for the detectors of X- and γ-radiation was continued, and the attention was attracted to another alloy on the basis of CdTe, $Cd_{1-x}Mn_xTe$.

While growing $Cd_{1-x}Mn_xTe$ crystals, the segregation phenomenon–one of the problems faced with in the technology of growing $Cd_{1-x}Zn_xTe$ – is less pronounced. In addition, for the bandgap in CdTe to be broadened to a required width, the amount of Mn which is to be introduced is approximately half as large as that of Zn. This allows the temperature to be lowered down, and the technological process to be made simpler and cheaper. The pioneer studies of $Cd_{1-x}Mn_xTe$ as a material for the detectors of X- and γ-radiation were made in the late 1990s [5]. The value of $\mu\tau$-product obtained for $Cd_{0.87}Mn_{0.13}Te$ crystals grown up following the Bridgman method was close to the record value obtained for the best CdTe specimens (more than 10^{-3} cm^2/V). The analysis of the isotope emission spectra registered by means of a detector fabricated in a different laboratory gave an $\mu\tau$-value by an order of magnitude smaller. Nowadays, the development of detectors on the basis of $Cd_{1-x}Mn_xTe$ are at the search stage. The results of researches carried out by well-known scientists and experts at leading laboratories confirm the progress in the development of such detectors and their promising capabilities [6, 7].

At the end of the 1990s, the Japanese authors published their results that revealed new possibilities of detectors on the basis of semiinsulating CdTe crystals with Schottky contacts and ultralow dark currents at high voltages [8, 9]. Soon, such detectors were used to achieve a high-energy resolution in the measurement of isotope spectra, in particular, in the region of quantum energies higher than 50 keV and inaccessible to silicon detectors. The companies leading in this domain refused to manufacture detectors on the basis of $Cd_{1-x}Zn_xTe$ (in spite of their higher resistivity and some other better parameters) and concentrated their efforts on detectors fabricated on the basis of CdTe with a Schottky diode [10]. These detectors started to be widely applied in science and engineering for carrying out the element analysis, in the gamma-beam spectroscopy, astrophysics, radiology, art, archeology, systems of nuclear monitoring, criminalistics, and so forth [11, 12]. The special attention is also attracted by multielement (pixel) image detectors, which are applied to medicine and engineering [13].

Nevertheless, despite the progress in technology, some issues concerning the physics of the processes governing the detection efficiency in CdTe crystals with a Schottky diode remain unrevealed. It is so because a detector fabricated on the basis of a sufficiently homogeneous CdTe crystal with a high resistivity, as well as with a large lifetime and a high mobility of charge carriers, is far from being always characterized by a proper detection efficiency and a required energy resolution. This is one of the main reasons of the fact that the fraction of manufactured devices suitable for applications turns out low, and the price of such devices is too high [14]. There emerges a hypothesis that some other characteristics of the material and the diode structure were not taken into account.

Certainly, the aforementioned requirements to the crystals used in detectors are obligatory. At the same time, the influence of the Schottky diode parameters – in particular, the SCR width – has not been considered in the literature. This is an evident fault because one cannot deny that the SCR width substantially affects the efficiency of X/γ-radiation de-

tection in a crystal with a Schottky diode, as well as in any barrier structure with photo-electric transformation (a photo diode, a solar cell). It is known that the SCR width in a diode structure is determined not by the concentration of free charge carriers in the semiconductor, but by that of noncompensated impurities. This means that the detection efficiency of X/γ-radiation depends on the compensation degree in the applied material. There is no theoretical analysis in the literature concerning the detection efficiency of X/γ-quanta in a crystal with a Schottky diode, which would be carried out making allowance for the influence of the SCR width, the recombination of charge carriers on the crystal surfaces, their capture in the SCR, and other factors on the collection of photogenerated charges. The elucidation of the mechanism of charge transfer in the Schottky diode fabricated on the basis of semiinsulating CdTe is also a challenging task. Its solution would not only allow the observed electric characteristics of the detector to be explained, but also the possibilities of their improvement to be revealed.

Below, the aforementioned physical aspects of the processes occurring in a CdTe-based detector with a Schottky diode are analyzed. The results published by the authors earlier [15–18] are summarized.

2. Electric Parameters of the Crystals

The detectors were fabricated with the use of chlorine-doped (to a concentration of about 10^{17} cm^{-3}) CdTe crystals (Acrorad Corporation). The technology of their growing was described in works [19, 20]. To measure the electric characteristics, specimens with a transverse cross-section of 2×0.5 mm^2 and a length of 5 mm were cut off from (111)-oriented wafers $5 \times 5 \times 0.5$ mm^3 in size. Ohmic contacts were deposited onto the end faces 2×0.5 mm^2 in size with the use of thermal sputtering of nickel in vacuum [8]. The current-voltage characteristic of such a prolate specimen was strictly linear, irrespective of the polarity of an applied voltage V within the interval from 0.1 to 100 V (the deviation from the linearity at $V > 100$ V is explained by the injection of electrons from the imperfect ohmic contact [16]). The magnitude of material resistivity was determined from the resistance found at low voltages and taking the geometrical dimensions of the specimen into account.

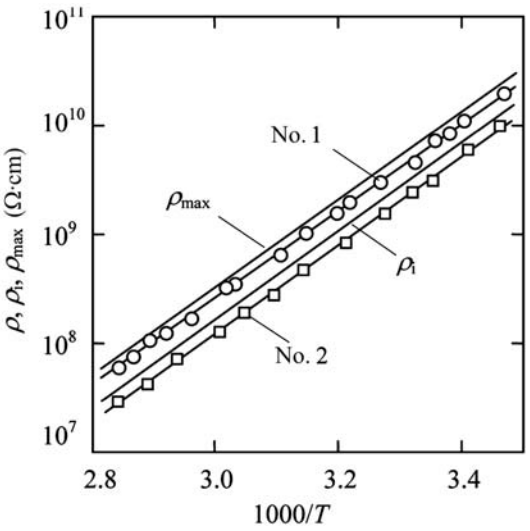

Fig. 1. Temperature dependences of the resistivity $\rho(T)$ for CdTe crystals (Nos. 1 and 2), the resistivity of CdTe with the intrinsic conductivity, $\rho_i(T)$, and the maximum resistivity, $\rho_{\max}(T)$

At a temperature of 300 K, the resistivity ρ of crystals amounted to $(3 \div 6) \times 10^9$ Ω·cm, which is close to the corresponding value for a material with intrinsic conductivity, $\rho = 4 \times 10^9$ Ω·cm, provided that the effective masses of electrons, m_n, and holes, m_p, equal $0.11m_0$ and $0.53m_0$, respectively [21–23], their mobilities $\mu_n = 1100$ cm^2/V·s and $\mu_p = 100$ cm^2/V·s [13], and the bandgap $E_g = 1.47$ eV [24].

2.1. Temperature dependence of resistivity

In Fig. 1, the typical temperature dependences of the resistivity, $\rho(T)$, for the examined crystals are depicted. For the sake of comparison, the temperature dependence of the resistivity for CdTe with the intrinsic conductivity, $\rho_{\rm i}(T) = 1/qn_{\rm i}(\mu_{\rm n} + +\mu_{\rm p})$, where $n_{\rm i} = (N_c N_{\rm v})^{1/2} \exp(-E_{\rm g}/2kT)$ is the concentration of charge carriers in the intrinsic CdTe, $N_{\rm c} = 2(m_{\rm n}kT/2\pi\hbar^2)^{3/2}$ and $N_{\rm v} = 2(m_{\rm p}kT/2\pi\hbar^2)^{3/2}$ are the effective density of states in the conduction and valence bands, respectively, of the semiconductor, and q is the electron charge, is also shown. From Fig. 1, one can see that the values of ρ and $\rho_{\rm i}$ are rather close to each other within the whole temperature interval, being different by no more than 20–30%. This fact is of importance with regard for our attempt to minimize the dark current in the X/γ-radiation de-

tectors. The observed excess of ρ over $\rho_{\rm i}$ is explained by a considerably lower mobility of holes in CdTe in comparison with that of electrons. If the Fermi level shifts from its position in the intrinsic semiconductor toward the valence band, the contribution of holes to the electric conductivity grows, and, consequently, the resistivity also increases. However, if the Fermi level shift continues to grow, the resistivity decreases, because the hole concentration becomes too high. Expressing ρ as $1/q(n\mu_{\rm n} + n_{\rm i}^2\mu_p/n)$ and equating the derivative $d\rho/dn$ to zero, it is easy to show that the maximum value of resistivity is determined by the expression

$$\rho_{\max} = \frac{1}{2qn_{\rm i}\sqrt{\mu_{\rm n}\mu_{\rm p}}}. \tag{1}$$

The temperature dependence $\rho_{\max}(T)$ is also exhibited in Fig. 1.

While calculating $\rho_{\rm i}$ and $\rho_{\max}$, the temperature dependence of the bandgap in CdTe (in electronvolts) [24] was taken into account,

$$E_{\rm g}(T) = 1.608 - 4.52 \times 10^{-4}T, \tag{2}$$

as well as the mobilities of electrons and holes,

$$\mu_{\rm n} = \mu_{n0}T^{-3/2}, \tag{3}$$

$$\mu_{\rm p} = \mu_{p0}T^{-3/2}. \tag{4}$$

In expressions (3) and (4), the temperature dependences of the electron and hole mobilities are described by the power function $T^{-3/2}$, because the scattering by optical phonons dominates in CdTe within the interval $T > 200$ K even at rather high impurity concentrations [25, 26]. The coefficients $\mu_{\rm n0}$ and $\mu_{\rm p0}$ were so selected that the mobility of electrons and holes be equal to 1100 and 100 $\rm cm^2/V \cdot s$, respectively, at room temperature [10].

The energy of thermal activation, ΔE, of the electric conductivity in researched CdTe crystals equals 0.792–0.795 eV. This value is close to that predicted by the theory and equal to half the bandgap at $T = 0$, i.e., according to formula (2), $\Delta E = 1.608/2 = 0.804$ eV. This result confirms, first, the ohmic character of the contacts with CdTe crystals and, second, the correctness of formula (2), which gives $E_{\rm g} = 1.47 \div 1.48$ eV at room temperatures (300 K and 20 °C). The latter fact is important, because the literature data on the bandgap in CdTe are too controversial. The values of $E_{\rm g}$ for CdTe crystals at 300 K quoted in various sources vary from 1.41 to 1.54 eV [24].

2.2. Fermi level energy and compensation degree in CdTe

The temperature dependence of the electric conductivity in semiinsulating CdTe – it is an important characteristic of the material intended to be used in detectors – is actually not discussed in the literature. Usually, it is asserted that the semiinsulating state arises in CdTe if a strongly compensated impurity creates a level in a vicinity of the energy gap middle point [27, 28]. This statement is somewhat inconsistent, because, by definition, the Fermi level coincides with the impurity level if the impurity compensation degree equals 50%, whereas it considerably moves away from the middle of the energy gap at a strong compensation, and, hence, the resistivity diminishes. Let us elucidate the position of the Fermi level and its temperature dependence in the examined crystals proceeding from the results of resistivity measurements and basing on the statistics of electrons and holes.

In the case of a semiconductor with the almost intrinsic conductivity, the energy distance between the Fermi level and the valence band top (hereafter, the Fermi level energy, $\Delta\mu$) can be determined by solving the equation for the resistivity, which looks in the general form as follows:

$$\rho(\Delta\mu) = \frac{1}{qn(\Delta\mu)\mu_{\rm n} + qp(\Delta\mu)\mu_{\rm p}}, \tag{5}$$

where the concentrations of electrons, $n(\Delta\mu)$, and holes, $p(\Delta\mu)$, in the conduction and valence, respectively, bands of a nondegenerate semiconductor are

$$n = N_{\rm c}\exp\left(-\frac{E_{\rm g} - \Delta\mu}{kT}\right), \tag{6}$$

$$p = N_{\rm v}\exp\left(-\frac{\Delta\mu}{kT}\right). \tag{7}$$

The solution of Eq. (5) for $\Delta\mu$ looks like

$$\Delta\mu = kT\ln\left(\frac{1 \pm \sqrt{1 - 4q^2\rho^2\mu_{\rm n}\mu_{\rm p}n_{\rm i}^2}}{2q\rho\mu_{\rm n}n_{\rm i}^2/N_{\rm v}}\right), \tag{8}$$

where the signs + and − are related to the electron and hole semiconductors, respectively.

In Fig. 2, the temperature dependence of the Fermi level energy, $\Delta\mu(T)$, calculated from the measured temperature dependence $\rho(T)$ (see Fig. 1) with the use of formula (8) for the hole type of material conductivity is shown. The same figure illustrates the position of the Fermi level in CdTe with the intrinsic conductivity found by the following formula, which makes allowance for the temperature dependence of the bandgap (2) [29]:

$$\Delta\mu_{\rm i}(T) = \frac{E_{\rm g}(T)}{2} + \frac{3}{4}kT\ln\left(\frac{m_{\rm p}}{m_{\rm n}}\right). \qquad (9)$$

As is seen from Fig. 2, the Fermi level is appreciably shifted toward the valence band from its position in the intrinsic semiconductor (by about 0.05 eV), i.e. the researched CdTe crystals have the p-type conductivity. This conclusion is also illustrated in Fig. 3 by plotting the ratio between the electron and hole concentrations calculated by formulas (6) and (7) and with the use of the found temperature dependence $\Delta\mu(T)$. One can see that the concentration of holes in the studied crystals exceeds the concentration of electrons by two to three orders of magnitude. We emphasize that the resistivity of the crystals differs only by 20–30% from that of CdTe with the intrinsic conductivity. Let us analyze how this state can be reached if the amount of uncontrollable impurities and defects is significant and, moreover, if CdTe is heavily doped with chlorine.

The consideration of the electron and hole statistics becomes simpler owing to a high concentration of chlorine in the examined crystals (higher that 10^{17} cm^{-3}), which considerably weakens the influence of uncontrollable ("background") impurities and defects, the concentration of which is substantial even in the purest and structurally perfect CdTe crystals [30–32]. The feature of doping with chlorine, as well as with other elements belonging to groups III and VII in the Periodic system, is known to consist in the formation of self-compensated complexes. The introduction of Cl atoms (a shallow impurity, as a rule) into CdTe induces the emergence of a deep donor level and a point defect (Cd vacancy), which plays the acceptor role. The effect of such a self-compensation was theoretically substantiated from the first principles in a series of works published as early as in the 1960s and confirmed in subsequent researches [33, 34].

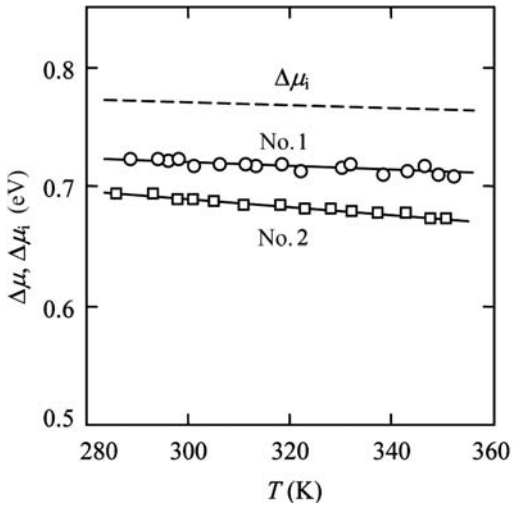

Fig. 2. Temperature dependences of the Fermi level energy $\Delta\mu$ in CdTe crystals (Nos. 1 and 2). The experimental results are denoted by circles and squares, and the results of calculation by formula (12) by solid curves. The dashed line demonstrates the position of the Fermi level $\Delta\mu_i$ in the intrinsic CdTe

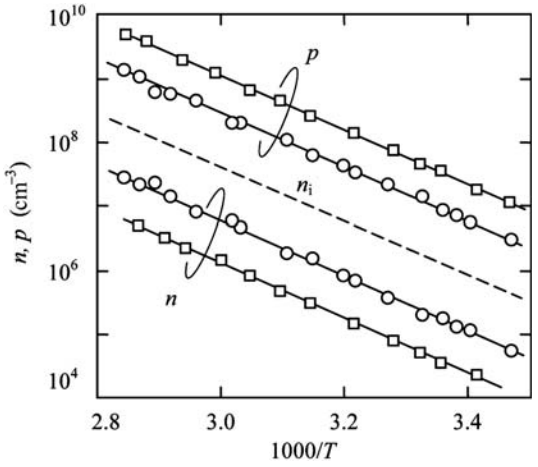

Fig. 3. Temperature dependences of the free electron and hole concentrations in CdTe crystals No. 1 (circles) and No. 2 (squares). The dashed line illustrates the concentration of charge carriers in the intrinsic CdTe

Provided that the doping with clorine plays a dominating role, the diagram of energy levels in the energy gap of CdTe is reduced to the presence of a single deep donor level and a single acceptor level, the both being associated with the formation of complexes. Some Cl atoms do not form complexes, and there emerges a shallow donor level in this case. This three-level

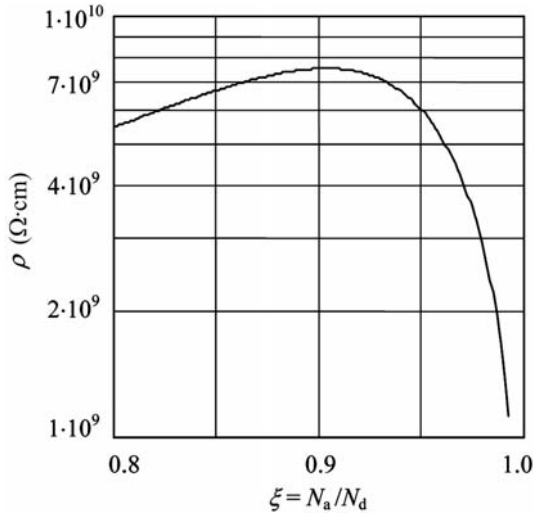

Fig. 4. Dependence of the resistivity ρ of a CdTe crystal at 300 K on the compensation degree ξ of a donor with an ionization energy of 0.68 eV and the level located at a distance of about 0.79 eV from the valence band

compensation model is applied to explain the semiinsulating conductivity in CdTe and CdZnTe crystals [35, 36]. The electroneutrality condition for the corresponding level diagram looks like

$$n + N_{\rm a}^{-} = p + N_{\rm dd}^{+} + N_{\rm sd}^{+}, \tag{10}$$

where, as before, n and p are the concentrations of free electrons and holes, respectively; and $N_{\rm a}^{-}$, $N_{\rm dd}^{+}$, and $N_{\rm sd}^{+}$ are the concentrations of charged acceptors, deep donors, and shallow donors, respectively.

Since the concentration of the doping impurity is high, the concentrations of free electrons and holes in Eq. (10) for the semiinsulating semiconductor can be neglected. Anticipating things, it should be noted that a strong self-compensation takes place at the doping with chlorine, so that the presence of shallow donors, the concentration of which is low because of this circumstance, can also be neglected. The acceptor levels are located in the lower half of the energy gap, being considerably removed from the Fermi level. Therefore, we may adopt that $N_{\rm a}^{-} \approx N_{\rm a}$, and Eq. (10) is reduced to the expression

$$\frac{N_{\rm dd}}{\exp\left(\frac{\Delta\mu - E_{\rm dd}}{kT}\right) + 1} = N_{\rm a}, \tag{11}$$

the solution of which for $\Delta\mu$ looks like

$$\Delta\mu = E_{\rm dd} + kT \ln\left(\frac{1-\xi}{\xi}\right), \tag{12}$$

where $E_{\rm dd}$ is the energy of a deep donor level, which is reckoned in this case, analogously to $\Delta\mu$, from the valence band top; and $\xi = N_{\rm a}/N_{\rm dd}$ is the degree of donor compensation by acceptors.

It is not difficult to confront expression (12) with the temperature dependence $\Delta\mu(T)$ found from the experimentally measured dependence $\rho(T)$ with the help of formula (8) and shown in Fig. 2 for two CdTe crystals with the help of circles and squares. The solid curve in Fig. 2 denotes the results of calculations by formula (12). The best agreement between the results of calculations and the experimental data was achieved for the following combinations of fitting parameters: $E_{\rm dd} = 0.792 \pm 0.02$ eV and $\xi = 0.95 \pm 0.005$ for crystal No. 1, and $E_{\rm dd} = 0.785 \pm 0.02$ eV and $\xi = 0.97 \pm 0.005$ for crystal No. 2.

The results obtained testify that the almost intrinsic conductivity in the studied CdTe crystals is provided by the same donor with the ionization energy $E_g - E_{dd} \approx 0.68$ eV and with the level located by 0.05–0.06 eV above the energy gap midpoint. Owing to the strong compensation, the Fermi level turns out below the energy gap midpoint, so that $\Delta\mu \approx 0.71$ eV for crystal No. 1 and $\Delta\mu \approx 0.69$ eV for crystal No. 2, both at 300 K. The difference between the $\Delta\mu$-values for two crystals is induced by the difference between the compensation degrees, $\xi = 0.95$ and 0.97. The results of calculation depicted in Fig. 4 illustrate the influence of the compensation degree ξ of this donor on the CdTe resistivity at 300 K. One can see that the maximum value $\rho_{\max} = 7.5 \times 10^9\ \Omega \times$ cm is reached at the compensation degree $\xi = 0.91$. If ξ increases, the resistivity ρ decreases, because the Fermi level shifts toward the valence band. At $\xi = 0.95$ and 0.97, $\rho = 6 \times 10^9$ and $3 \times 10^9\ \Omega \times$ cm, respectively.

It should be noted that the semiinsulating state can also be realized in the case where the donor level is located considerably far from the energy gap midpoint. However, it can happen at higher compensation degrees.

3. Electric Parameters of Schottky Diodes

Detectors with a Schottky diode were fabricated by sputtering Ni in vacuum onto the preliminarily

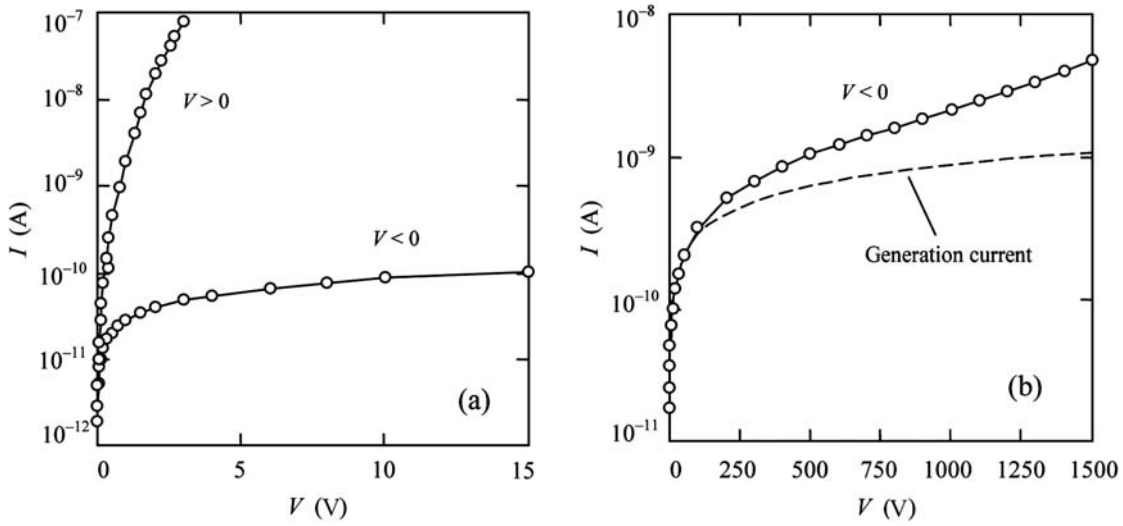

Fig. 5. (*a*) $I - V$ characteristic of a Ni/CdTe/Ni detector at low voltages and (*b*) the reverse current in a wide voltage interval at 300 K

treated (111)-oriented surface of a CdTe wafer $5 \times 5 \times$ $\times 0.5$ mm^3 in size [16]. The area of Schottky contacts was $3.16 \times 3.16 = 10$ mm^2. A Ni ohmic contact was deposited onto the opposite surface of the wafer. The procedure of the ohmic and Schottky contact formation included the chemical and ionic (Ar) etchings of the crystal surface. The qualitative difference between the properties of contacts at the opposite wafer surfaces is explained, first, by the application of different, CdTe(111)B and CdTe(111)A, surfaces and, second, by the changes in the system of surface electron states owing to different regimes of chemical and ionic surface etchings. Due to a high concentration of surface states in CdTe crystals, the difference between the work functions and the electron affinities of the materials does not play a crucial role in the contact formation.

Diode structures with the Ni/CdTe/Ni contact are characterized by rather high rectifying properties and low reverse currents, which enables the application of a high inverse voltage (up to 1500–2000 V) to them. As is seen from Fig. 5, the rectification factor at a voltage of about 3 V exceeds 10^3 and can grow further by several orders of magnitude if the voltage increases. Such a high rectification factor in the presence of a large series resistance of the crystal bulk section (of about 10^9 Ω) is explained by the injection of minority charge carriers (electrons) at the forward connection of the Schottky contact to the neutral section of the crystal and the resulting modulation of its conductivity [17]. The effect manifests itself so strongly because of a low concentration of free charge carriers in CdTe with the almost intrinsic conductivity ($p \approx 10^6$ cm^{-3}).

If the Ni/CdTe/Ni structure is connected in the reverse direction, charge carriers are not injected from the Schottky contact, and the current I grows sublinearly, as the voltage increases (at $V < 100 \div 200$ V). As the voltage V increases further, the current–voltage dependence transforms into a linear one, but, at voltages higher than 1000 V, a superlinear growth of the current, which is highly undesirable for a detector, is observed. The origin of this phenomenon consists in that the applied technology of Ni (as well as Au or Pt) deposition does not allow one to obtain an ideal ohmic contact with "flat" bands near the crystal surface. In a real "ohmic" contact, the band bending takes place in the near-surface layer, which is similar to that in the Schottky contact, but is much smaller [17]. As the reverse current increases, some fraction of the applied voltage drops down not only across the crystal bulk, but across the "ohmic" contact as well. As a result, the potential barrier decreases, which gives rise to the injection of charge carriers into the neutral section of the crystal. Diffusion of those carriers to the Schottky contact is summed up with their drift under the influence of the electric field emerging owing to the voltage drop across

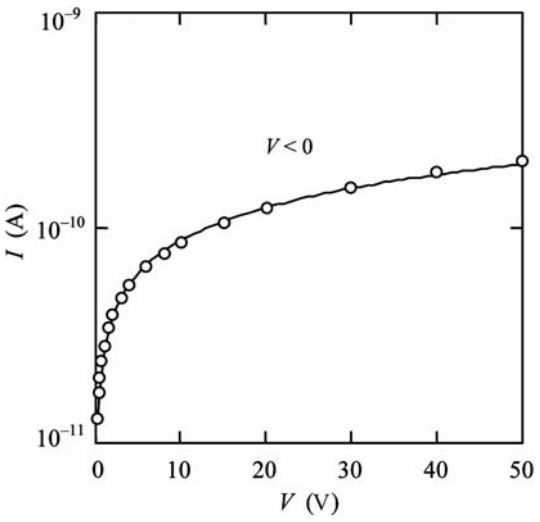

Fig. 6. Comparison between the reverse experimental I–V characteristic of the Ni/CdTe/Ni detector (circles) and the results of calculations according to the Sah–Noyce–Shockley theory (300 K)

the resistance of the crystal bulk. All those factors favor the penetration of injected charge carriers into the barrier region of the reversely biased Schottky contact and the additional increase of the current in the external circuit. Hence, an insufficient quality of the ohmic contact in a CdTe detector with a Schottky diode gives rise to the increase of the dark current through the Ni/CdTe/Ni structure at elevated reverse voltages [17].

At relatively low voltages, the reverse I–V characteristic of the Ni/CdTe/Ni detector is described by the Sah–Noyce–Shockley theory of generation-recombination in the SCR developed for a $p-n$ junction [37]. According to this theory, the rate of generation-recombination in the SCR cross-section x at the voltage V is determined by the expression

$$U(x,V)=\frac{n(x,V)p(x,V)-n_{\rm i}^2}{\tau_{\rm n0}[n(x,V)+n_1]+\tau_{\rm p0}[p(x,V)+p_1]}, \quad (13)$$

where $n(x,V)$ and $p(x,V)$ are the concentrations of charge carriers in the SCR in the conduction and valence bands, respectively; $\tau_{\rm n0}$ and $\tau_{\rm p0}$ are the effective lifetimes of electrons and holes, respectively, in the SCR; and the quantities n_1 and p_1 are determined by the depth of the generation-recombination level $E_{\rm t}$ (the energy distance from the valence band edge: $n_1 = 2(m_{\rm n}kT/2\pi\hbar^2)^{3/2}\exp[-(E_{\rm g}-E_{\rm t})/kT]$ and $p_1 = 2(m_{\rm p}kT/2\pi\hbar^2)^{3/2}\exp[-E_{\rm t}/kT]$.

The recombination current at the forward bias voltage and the generation current at the reverse one are determined by integrating $U(x,V)$ over the whole depleted layer (A is the diode area),

$$I = Aq\int_0^W U(x,V)dx. \quad (14)$$

In the Sah–Noyce–Shockley theory adapted for the Schottky diode and in the chosen reference frame, the expressions for the electron and hole concentrations look like [38]

$$n(x,V) = N_{\rm c}\exp\left[-\frac{E_{\rm g}-\Delta\mu-\varphi(x,V)-qV}{kT}\right], \quad (15)$$

$$p(x,V) = N_{\rm v}\exp\left[-\frac{\Delta\mu+\varphi(x,V)}{kT}\right], \quad (16)$$

where $\Delta\mu$ is the energy distance of the Fermi level in the CdTe bulk, and the potential energy $\varphi(x,V)$ for the Schottky diode looks like $\varphi(x,V) = (\varphi_0 - qV)(1-x/W)^2$, where φ_0 is the barrier height from the semiconductor side, W is the SCR width determined by the formula [39]

$$W = \sqrt{\frac{2\varepsilon\varepsilon_0(\varphi_0-qV)}{q^2N}}, \quad (17)$$

in which ε is the relative permittivity of a semiconductor, ε_0 the electric constant, and N the concentration of noncompensated impurities.

The results of calculations of the I–V characteristic, by using formula (14) and taking Eqs. (13) and (15)–(17) into account, are shown in Fig. 6 by a solid curve (300 K). The parameters of calculations are $\Delta\mu = 0.72$ eV, $\varphi_0 = 0.6$ eV, depth of the generation-recombination level $E_t = 0.78$ eV, and concentration of noncompensated impurities $N = 2\times10^{12}$ cm^{-3}. To provide the best coincidence between the results of calculations and the experimental data, the lifetimes of electrons and holes in the depleted layer, $\tau_{\rm n0}$ and $\tau_{\rm p0}$, respectively, had to be put equal to 3×10^{-8} s. The values for the parameters N, $\tau_{\rm n0}$, and $\tau_{\rm p0}$ were chosen, by basing on the reasons discussed in Section 4. The excellent agreement between the results of calculations and experimental data, which

is illustrated in Fig. 6, confirms the proper choice of the physical model for processes that occur in the Ni/CdTe/Ni structure.

The model of generation-recombination processes in the SCR adequately describes not only the current dependence on the voltage, but also the temperature-induced variations in the diode I–V characteristic. According to the Sah–Noyce–Shockley theory, the temperature dependence of the generation current is expressed by the quantity $T^{3/2}\exp(-\Delta E/kT)$, i.e. the activation energy ΔE can be determined from the slope of the dependence $\log(I/T^{3/2})$ versus $1000/T$, as is shown in Fig. 7. It is reasonable to suppose that the generation of charge carriers occurs through levels belonging to complexes that are formed as a result of the chlorine doping. The concentration of these complexes is much higher than that of background impurities (defects). Really, the impurity (defect) ionization energy $E_{\rm t}$ fitted to provide the best coincidence between the results of calculations and the experimental results equals 0.78 eV, which is very close to the deep donor ionization energy given above, $E_{\rm dd} = 0.792$ eV.

At voltages higher than about 100 V, the registered current starts to appreciably exceed the generation current (approximately by a factor of five at 1500 V). For the interpretation of charge transfer mechanisms in a wide voltage interval, it is convenient to present the I–V characteristic on the log-log scale (Fig. 8). One can see that a root dependence is clearly observed in the dependence $I(V)$ at $V \lesssim 100$ V. It is quite clear, because, according to the Sah–Noyce–Shockley theory of generation-recombination in the SCR, if the reverse voltage satisfies the condition $qV \gg kT$, the multiplier $[\exp(qV/2kT) - 1]$ does not reveal itself (at reverse voltages, $V < 0$) and the dependence of I on V becomes root-like ($I \sim V^{1/2}$).

However, at $V \gtrsim 100$ V, the mechanism of conductivity changes, and the dependence $I(V)$ becomes linear in the V-interval from about 200 to 800–900 V, which explicitly manifests itself as a constant differential resistance in this voltage interval [16]. Such a behavior of the I–V characteristic is explained by the peculiarities of the charge transfer process in CdTe under the action of a strong electric field. Really, at $V = 500$ V and a crystal thickness of 0.5 mm, the electric field strength in the crystal equals 10^4 V/cm, and the mobility of charge carriers in CdTe starts to depend on the electric field, so that if V increases,

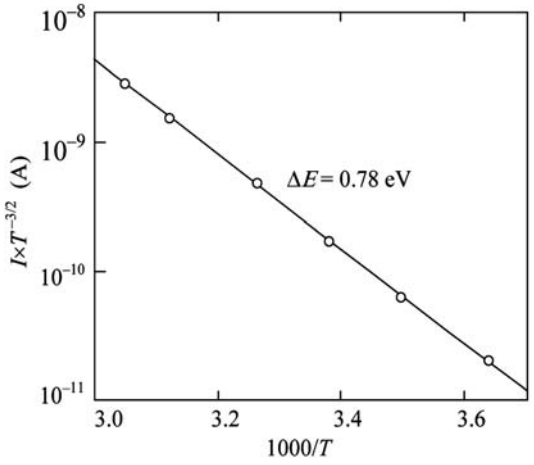

Fig. 7. Temperature dependence of the reverse current in the Ni/CdTe/Ni detector at $V = 50$ V

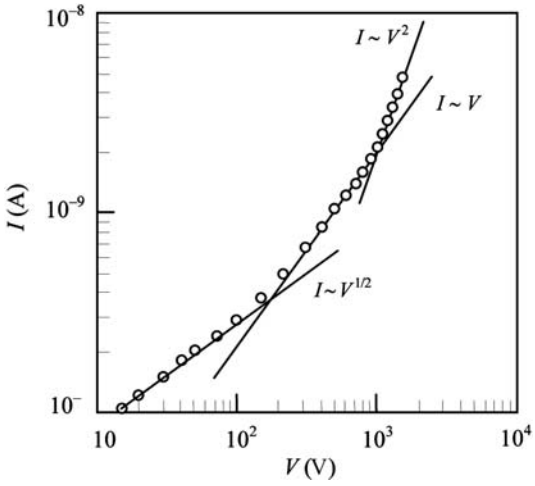

Fig. 8. Reverse I–V characteristic of the Ni/CdTe/Ni structure on the log-log scale. Approximations of the root ($I \sim V^{1/2}$), linear ($I \sim V$), and square-law ($I \sim V^2$) current dependences on the voltage are shown

the velocity of charge carriers saturates at a level of about 10^7 cm/s [40]. This regime of charge transfer is known to give rise to a linear current dependence on the voltage ($I \sim V$) [39]. At last, at even higher voltages, the regime of the current restricted by the bulk charge takes place. At $V \gtrsim 1100$ V, the current becomes proportional to the squared voltage ($I \sim V^2$), i.e. the Mott–Gurney law [39] is obeyed.

Hence, the reverse I–V characteristic of the Ni/CdTe/Ni structure can be described in the framework of known theoretical models in the whole range

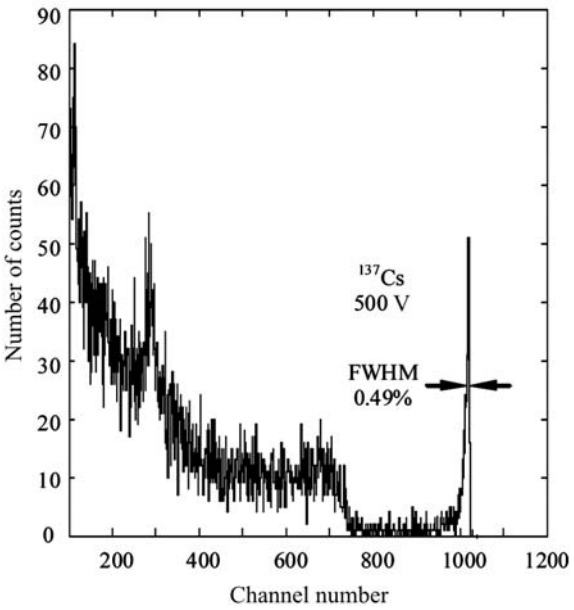

Fig. 9. Radiation emission spectrum of ^{137}Cs isotope obtained at a voltage of 500 V across the detector

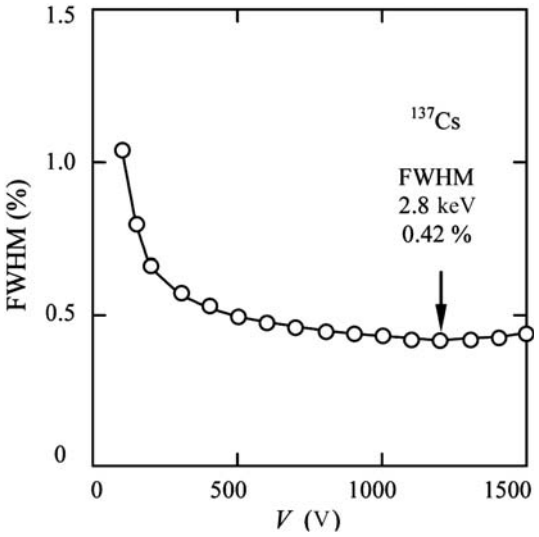

Fig. 10. Dependence of the line half-width in the spectrum of ^{137}Cs isotope on the voltage applied to the detector

of voltage variation. Note that the voltage at which an undesirable drastic growth of the current is observed ($I \sim V^2$) depends on the technology of "ohmic" contact deposition. The energy diagram of the latter, as was already marked above, is similar to that in the Schottky contact, but with a smaller band bending [17]. At high voltages, electrons are injected from this contact into the neutral part of the crystal and, then, into the SCR of the Schottky contact.

4. Energy Resolution and Efficiency of Detector with Schottky Diode

4.1. Energy resolution

Low reverse currents at high voltages (by an order of magnitude smaller in comparison with a crystal of the same dimensions but with ohmic contacts) allowed the detection efficiency and the energy resolution of CdTe crystals with a Schottky diode to be improved. This is confirmed by the results of measurements of the ^{137}Cs isotope spectrum obtained with the help of one of Ni/CdTe/Ni detectors (see Fig. 9). The spectra were measured with the use of a charge-sensitive amplifier CP-5102 BS in combination with a multichannel analyzer MCA7600.

First of all, the attention is drawn to a high energy resolution of the line at 662 keV in the spectrum depicted in Fig. 9. The line full width at half maximum (FWHM) amounts to 3.2 keV, which corresponds to 0.49% of the photon energy in the radiation emitted by ^{137}Cs isotope (the corresponding values at a voltage of 1200 V are 2.8 keV and 0.42%). This resolution is higher than the FWHM values quoted in the literature, e.g., by the Amptek Inc. company, one of the world leaders in the manufacture of CdTe detectors; in particular, FWHM = 0.89% at room temperature [41]. Till now, a higher energy resolution for the 662-keV line was achieved only when a CdTe detector was cooled down to -70 °C (FWHM = 0.32%) [42] or with the help of a germanium detector at nitrogen temperatures (FWHM = 0.2%) [43].

The dark current in the Ni/CdTe/Ni detector is extremely low, which gives a possibility to apply a high voltage. In this case, the strong electric field existing in CdTe provides a high charge collection efficiency and, hence, a high energy resolution of the detector, which is illustrated in Fig. 10. The dependence of FWHM on V with a minimum, which is exhibited in this figure, can be explained by a competition of two processes. The charge collection efficiency grows, as the voltage V increases from the lowest values, which is accompanied by a reduction of the line half-width. A slowing-down of its reduction at voltages higher than about 500 V is explained by the fact that the charge collection becomes as complete as possible (be-

cause the electric field strength amounts 10^4 V/cm at a crystal thickness of 0.5 mm and $V = 500$ V). At the same time, the increase of V is accompanied by the growth of the dark current in the detector circuit, and the negative influence of this current on the line half-width becomes appreciable at voltages higher than about 1200 V.

Besides the 662-keV line, the ^{137}Cs spectrum contains an intensive broadband radiation with photon energies $h\nu < 480$ keV (Fig. 9). It is explained as an intensive Compton scattering of photons with an energy of 662 keV.

4.2. Influence of the space charge region width on the detection efficiency

An expression for the quantum efficiency of the detection of X- and γ-quanta by a Schottky diode can be obtained by solving the continuity equation with the corresponding boundary conditions. The exact solution of this equation, which makes allowance for the drift and diffusion components of the quantum efficiency, as well as the recombination on the crystal surfaces, is described by cumbersome expressions including components that are expressed in terms of integral functions [44]. However, the problem can be considerably simplified, if we consider the specific features of the processes running in X- and γ-detectors created on the basis of semiinsulating CdTe.

As was already mentioned, the application of CdTe is especially important owing to a possibility to detect X- and γ-quanta with high energies, for which the absorption factor α_γ is rather low [45]. The results of calculations made for the drift component of the detection efficiency and reported in our work [17] testify that the recombination on the crystal front surface practically does not affect the detection efficiency if $\alpha_\gamma < 10^3$ cm^{-1}, i.e. for photon energies $h\nu \gtrsim 10$ keV. At $h\nu < 10$ keV, i.e. at $\alpha_\gamma > 10^3$ cm^{-1}, the recombination losses on the front surface become appreciable, gradually increasing to 15–16% at $h\nu = 1$ keV. Therefore, while calculating the spectra of such widespread isotopes as ^{55}Fe (5.9 keV), ^{241}Am (59.54 keV), ^{57}Co (122 keV), ^{133}Ba (356 keV), and ^{137}Cs (662 keV), there is no necessity to take the recombination of charge carriers on the front crystal surface into account. However, if doing so, it is necessary to consider their capture (trapping) in the SCR of studied Schottky diodes fabricated on the basis of semiinsulating crystals. First, the SCR in those diodes is rather wide even at the zero bias, so that the electric field strength is relatively low at moderate voltages. Second, the lifetimes of electrons, τ_{n0}, and holes, τ_{p0}, in the SCR are much shorter than those in the neutral section of the crystal (see Subsection 4.3). This means that the drift lengths of electrons, $\lambda_n = \tau_{n0}\mu_n E$, and holes, $\lambda_p = \tau_{p0}\mu_p E$–here, E is the electric field strength in the SCR, and μ_n and μ_p are, as before, the mobilities of electrons and holes, respectively–can be comparable and even less than the SCR width.

The capture of charge carriers in the SCR can be taken into account by using the well-known Hecht equation [46],

$$\eta_H(x) = \frac{\lambda_n}{W}\left[1 - \exp\left(-\frac{x}{\lambda_n}\right)\right] + \frac{\lambda_p}{W}\left[1 - \exp\left(-\frac{W-x}{\lambda_p}\right)\right], \quad (18)$$

where x is the coordinate, where the electron-hole pair was created.

In a Schottky diode, the electric field is nonuniform. However, since the field strength decreases linearly with the coordinate x, then, it can be substituted by its averaged values in the sections $(0, x)$ and (x, W) in the expressions for λ_n and λ_p; namely, $(\varphi_0 - qV)(2 - x/W)/qW$ and $(\varphi_0 - qV)(1 - x/W)/qW$, respectively [15]. Then, taking the aforesaid into account, the drift component of the detection efficiency by a Schottky diode looks like

$$\eta_{dr} = \int_0^W \eta_H(x)\alpha_\gamma \exp(-\alpha_\gamma x)dx. \quad (19)$$

Here, it was assumed that the rate of electron-hole pair generation by photons with the coefficient of photo-electric absorption α_γ in the cross-section x of the SCR is equal to $\alpha_\gamma \exp(-\alpha_\gamma x)$ [39].

The expression for the diffusion component of the detection efficiency can also be considerably simplified by neglecting the recombination on the back surface of the crystal. This simplification is reasonable, because the photo-electric absorption factors for photons with high energies are so low (e.g., $\alpha_\gamma \approx \approx 0.1$ cm^{-1} for ^{137}Cs) that the excitation of electron-hole pairs can be regarded as almost uniform over the

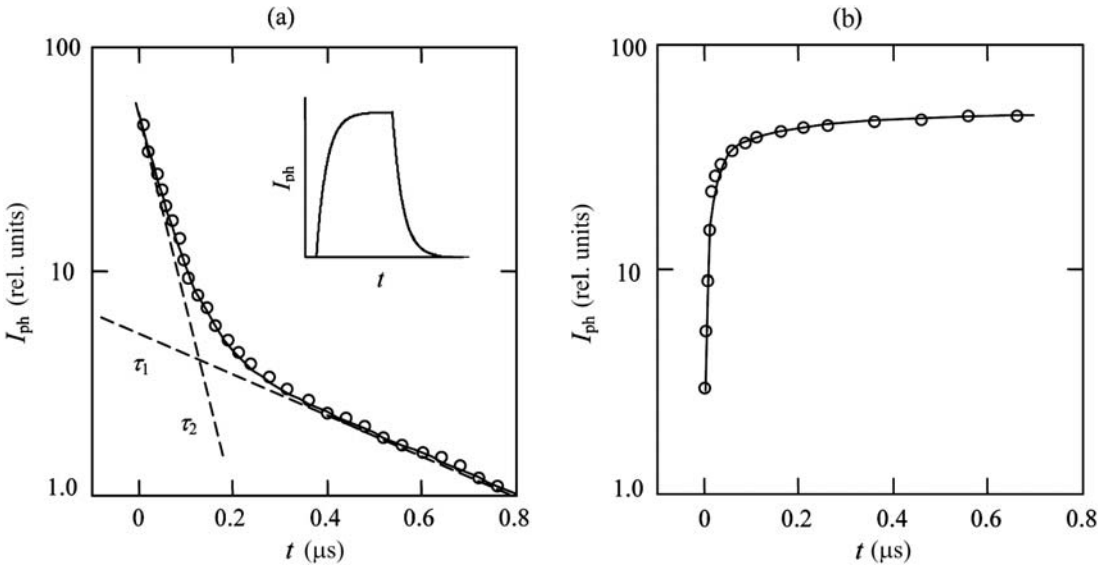

Fig. 11. Recession (a) and growth (b) curves of the photocurrent excited with semiconductor laser pulses ($\lambda = 782$ nm) in the Ni/CdTe/Ni detector. The experimental and calculated results are denoted by circles and solid curves, respectively. The inset demonstrates the example of a photocurrent oscillogram

whole crystal. Under those conditions, the recombination on the back surface practically does not make contribution, because it occurs in a layer with the thickness amounting to a small fraction of the crystal thickness. For isotopes with low energies of emitted photons, the absorption factor is much higher, but only a small fraction of the incident radiation reaches the back surface, i.e. the recombination effect can also be neglected in this case.

If the recombination on the back crystal surface is ignored, the solution of the continuity equation gives the diffusion component of the detection efficiency in the form $\alpha_\gamma L_\mathrm{n} \exp(-\alpha_\gamma W)/(1 + \alpha_\gamma L_\mathrm{n})$, where the multiplier $\exp(-\alpha_\gamma W)$ makes allowance for the radiation attenuation while passing through the SCR [15]. Since the electrons generated in the neutral section of the crystal enter the SCR at the coordinate $x = W$, the losses associated with the capture of charge carriers can be taken into account, by multiplying the expression for the diffusion component given above by $\eta_\mathrm{H}(W)$. Hence, the detection efficiency in the examined Ni/CdTe/Ni structure irradiated from the Schottky contact side can be calculated by the formula

$$\eta = \int_0^W \eta_\mathrm{H}(x)\alpha_\gamma \exp(-\alpha_\gamma x)dx + \frac{\alpha_\gamma L_\mathrm{n}}{1+\alpha_\gamma L_\mathrm{n}} \exp(-\alpha_\gamma W)\eta_\mathrm{H}(W). \quad (20)$$

4.3. Lifetime of charge carriers in the SCR of analyzed Schottky diodes

In order to calculate the detection efficiency η, we have to know the lifetimes of charge carriers in the SCR, because those quantities enter the expressions for λ_n and λ_p in formula (18). Our researches of the relaxation curves describing the growth and the recession of a photocurrent at its excitation by rectangular pulses emitted by a semiconductor laser ($\lambda = 782$ nm) showed that the lifetimes of charge carriers are drastically different in the SCR and in the neutral section of the CdTe crystal. In the case of a crystal with two ohmic contacts, the lifetime of electrons amounts to a few microseconds, which agrees with the data presented at the Web site of Acrorad Co. Ltd. [47]. At the same time, if the crystal is irradiated through the translucent Schottky contact, the radiation with a wavelength of 782 nm is absorbed in a thin near-surface layer of the SCR. This means that it is just the lifetime of charge carries in the SCR that can be determined from the photocurrent relaxation curves.

In Fig. 11, the curves of the growth and the recession of a photocurrent in the Ni/CdTe/Ni struc-

ture are presented at an applied voltage of 1000 V, which is close to the optimum value for the detection efficiency and the energy resolution. In our studies, the laser pulse duration was varied from 100 to 1000 ns, the reciprocal pulse ratio (the ratio between the pulse period and the pulse duration) from 100 to 1000, and the unfocused laser beam power in a pulse from 1 to 10 mW.

The recombination of photo-generated charge carriers occurs through the impurity and defect levels, and their lifetime depends not only on the concentration and the capture cross-section of impurities (defects), but also on their charge state, which depends, in turn, on the position of the impurity (defect) level relative to the Fermi quasilevel in the SCR. In practice, it is the averaged (effective) lifetime of charge carriers in the SCR that manifests itself and depends not only on the material parameters, but also on the excitation conditions.

One can assume that the curve $I_{\rm ph}(t)$ reflecting the photocurrent recession that occurs after the laser irradiation termination is described by the function $\exp(-t/\tau)$, where τ is the lifetime of charge carriers. Sometimes, this dependence is really observed, and the behavior of $I_{\rm ph}(t)$ on the logarithmic scale is described well by a straight line. However, in the overwhelming majority of cases, the photocurrent recession curve cannot be approximated by a single exponential function. Instead, its time profile can be described very well if we suppose that there exist two processes with different lifetimes: short, τ_1, and long, τ_2, ones, the lifetime for the latter being approximately 10 times as large (Fig. 11, *a*). According to this model of photocurrent recession, we may write down

$$I_{\rm ph}(t) = I_1 \exp\left(-\frac{t}{\tau_1}\right) + I_2 \exp\left(-\frac{t}{\tau_2}\right), \qquad (21)$$

where I_1 and I_2 are coefficients depending on the concentration of capture centers.

In the simplest case, the photocurrent growth curve should be described by the function $1 - \exp(-t/\tau)$. However, a satisfactory agreement between the experimental curve and this theoretical dependence is not reached. At the same time, an agreement is obtained if a participation of two processes is supposed, i.e. if the photocurrent growth is described by the expression

$$I_{\rm ph}(t) = I_1\left[1-\exp\left(-\frac{t}{\tau_1}\right)\right] + I_2\left[1-\exp\left(-\frac{t}{\tau_2}\right)\right], \qquad (22)$$

which is confirmed by a comparison of experimental data with the results of calculations by this formula (Fig. 11, *b*). The average lifetimes determined from the measured photocurrent curves equal $\tau_1 = (2 \div 5) \times 10^{-8}$ s $\approx 3 \times 10^{-8}$ s and $\tau_2 = (2 \div 4) \times 10^{-7}$ s $\approx 3 \times 10^{-7}$ s. Under the conditions, when a high constant voltage is applied to the detector, the effective lifetime of charge carriers in the SCR, τ, seems to be closer to the lower value. The analysis of the results obtained for several detectors testifies that the lifetime concerned is approximately equal to 3×10^{-8} s.

4.4. Comparison of the results of calculations for the detection efficiency with experimental data

The results of calculations of the dependence of the quantum detection efficiency η on the concentration N of noncompensated impurities for the radiation emitted by ^{137}Cs isotope ($h\nu = 662$ keV and $\alpha_\gamma = 0.1$ cm^{-1}) are depicted in Fig. 12. At calculations, the lifetime of electrons in the neutral section of a CdTe crystal was taken to equal 10^{-6} s, and the lifetimes of electrons and holes in the SCR $\tau_{\rm n0} = \tau_{\rm p0} = 3 \times 10^{-8}$ s. Typical values were taken for other parameters, and the voltage applied to a detector was 400 V.

As is seen from Fig. 12, the dependence of η on N is described by the curve with a strongly pronounced maximum. The maximum in the dependence $\eta(N)$ is observed at a concentration of noncompensated impurities of about 2×10^{11} cm^{-3}. The calculations show that, for lower photon energies, the maximum position shifts, although slightly, toward higher concentrations of noncompensated impurities [18].

The results depicted in Fig. 12 have an important practical value. They imply that, besides the material uniformity, high resistivity, large lifetime, and high mobility of charge carriers, one more requirement to the detector material is put forward; this is a definite concentration of noncompensated impurities. This parameter should not be identified with the concentration of free charge carriers (in the case of CdTe, these are holes in the valence band); the both can differ from each other by several orders of magnitude.

The SCR width can evidently depend not only on the concentration of noncompensated impurities

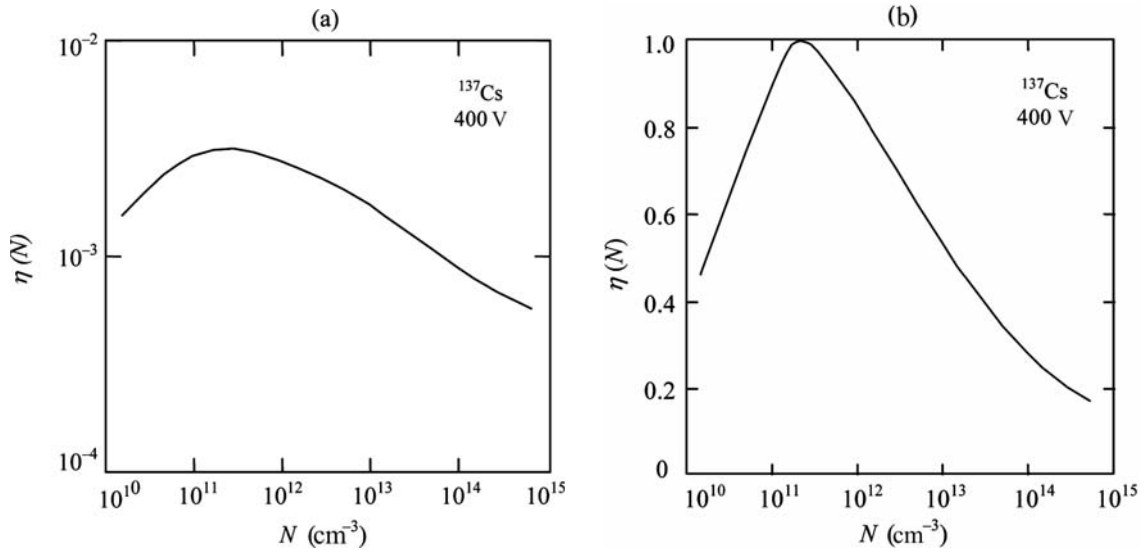

Fig. 12. (a) Dependence of the detection efficiency η of 662-keV photons (^{137}Cs isotope) by a CdTe crystal with a Schottky diode on the concentration of noncompensated impurities N calculated by formula (20) and (b) the same dependence normalized by the maximum value

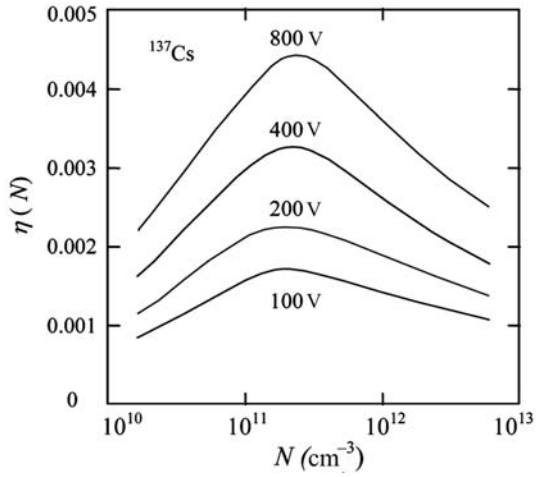

Fig. 13. Dependences of the detection efficiency of the CdTe crystal with a Schottky diode on the concentration of noncompensated impurities N calculated by formula (20) for various voltages

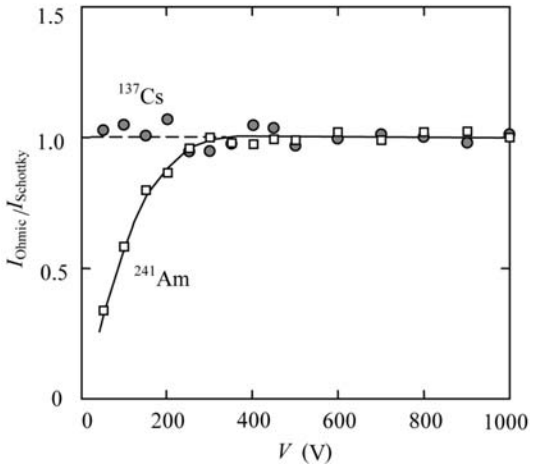

Fig. 14. The ratios between the peak heights in the spectra of ^{137}Cs and ^{241}Am obtained at the specimen irradiation from the ohmic and Schottky contact sides as functions of the voltage applied to a detector

but also on the voltage applied to a detector. However, according to the calculated results exhibited in Fig. 13, the voltage practically does not affect the positions of maxima in the curves $\eta(N)$. As is seen from this figure, an increase of the voltage by almost an order of magnitude results in a slight shift of the maximum toward higher N-values. Such a behavior of the dependence $\eta(N)$ can be explained, to a great extent, by the fact that the electron (hole) transit time through the SCR in a Schottky diode does not depend on the applied voltage. Really, the average value of the electric field strength in the SCR is equal to $(\varphi_0 - qV)/qW$, so that the average velocity of electrons at their passage through the SCR is

$\mu_n(\varphi_0 - qV)/qW$. Dividing W by the latter quantity, we obtain the electron transit time through the SCR,

$$t_{tr} = \frac{2\varepsilon\varepsilon_0}{q\mu_n N}, \quad (23)$$

i.e. a value independent of the voltage, but reciprocal to N.

The SCR width in the examined Schottky diodes can be determined by comparing the spectra of ^{137}Cs and ^{241}Am isotopes obtained at the irradiation of the detector from the Schottky and ohmic contact sides. In the case of isotopes with a high photon energy, e.g., ^{137}Cs, the generation of electron-hole pairs can be regarded as almost uniform within the whole crystal volume (this circumstance was already mentioned above). Really, the absorption factor of the ^{137}Cs isotope radiation associated with the photoeffect equals about 0.1 cm^{-1} [45]. This means that the effective depth of radiation penetration into CdTe is equal to about 10 cm. Obviously, the height of the ^{137}Cs isotope line should not depend on which side of the specimen is irradiated (absorption in the nickel film with the micron-sized thickness can be neglected at a photon energy of 662 keV).

A different scenario should be observed if ^{241}Am isotope is used. The absorption factor for its radiation is equal to approximately 40 cm^{-1}, and the effective depth of radiation penetration into CdTe is about 250 μm. In this case, if the crystal thickness equals 0.5 mm, the radiation is attenuated by approximately a factor of seven. One may expect that, under such a condition of non-uniform generation of electron-hole pairs, the line height in the ^{241}Am spectrum should depend on which side of the detector is irradiated. Moreover, it must differently depend on the voltage applied to the detector, especially if the SCR occupies an insignificant part of the crystal thickness.

Let I_{ohm} and I_{sch} denote the peak heights in the spectra obtained with the help of a CdTe detector irradiated from the ohmic and Schottky, respectively, contact sides. In Fig. 14, the experimental dependences of the ratio I_{ohm}/I_{sch} on the voltage are shown in the cases of irradiation with the use of ^{137}Cs and ^{241}Am isotopes. One can see that the peak-height ratio for ^{137}Cs isotope remains close to 1 within the whole interval of voltages V applied to the detector down to its lowest values (50–100 V). For ^{241}Am isotope, the ratio I_{ohm}/I_{sch} is much less than 1 at low V, but grows with V. However, at $V = 350 \div 400$ V, the ratio I_{ohm}/I_{sch} reaches 1 and does not change if the voltage grows further. It is reasonable to suppose that, at voltages of 350–400 V, the SCR width is equal to the crystal thickness, $d = 0.5$ mm. Then, according to formula (15), the concentration N of noncompensated impurities turns out close to 10^{12} cm^{-3} ($\varepsilon = 10.9$, and φ_0 is neglected at such a high voltage). At $N = 10^{12}$ cm^{-3}, $V = 0$, and $\varphi_0 = 0.3 \div 0.7$ eV, the SCR width equals 20–30 μm, i.e. it is a small fraction of the crystal thickness.

Hence, the concentration of noncompensated impurities $N \approx 10^{12}$ cm^{-3} in the analyzed crystals turns out to be rather close to the optimum one (2×10^{11} cm^{-3}) needed for an effective detection of the radiation emitted by ^{137}Cs isotope (see Fig. 14). This circumstance explains the observed high resolution in the spectrum of this isotope.

5. Conclusions

The electric properties of chlorine-doped CdTe single crystals with the conductivity close to the intrinsic one, the electric characteristics of Ni/CdTe/Ni structures with a Schottky diode, detection efficiency, and energy resolution of the radiation spectra of isotopes with the energy of gamma quanta $h\nu > 10$ keV have been studied.

1. The analysis of the charge-carrier statistics in the framework of the model of self-compensated complexes that emerge, when CdTe is doped with chlorine allowed not only the electric parameters of the crystals to be explained, but also the ionization energy and the compensation degree of a doping impurity, which plays a crucial role in the detector functioning, to be determined.

2. The current-voltage characteristics of the Ni/CdTe/Ni structure are described by the Sah–Noyce–Shockley generation-recombination theory (at voltages lower than about 100 V), by the charge transfer mechanism in the regime of charge-carrier velocity saturation (at voltages from 200 to 600–700 V), and by the mechanism of current restriction by the space charge (at voltages higher than about 1100 V).

3. The efficiency of the detection of X/γ-quanta in CdTe crystals with a Schottky diode was considered theoretically with regard for the influences of the SCR width, the recombination of charge carriers on the crystal surfaces, and their capture in the SCR. The dependence of the γ-quantum detection efficiency on

the concentration of noncompensated impurities, N, was found to be described by a function with a maximum (at $N \approx 2 \times 10^{11}$ cm^{-3} for the ^{137}Cs line).

4. The Ni/CdTe/Ni structures with a Schottky diode and have an energy resolution of 0.42% in the spectrum of ^{137}Cs at a voltage of 1200 V (300 K). These parameters are provided by low dark currents at high voltages and an almost optimal value of the concentration of noncompensated impurities (of about 10^{12} cm^{-3}) in the applied CdTe crystals.

The research was carried out in the framework of the joint international project COCAE SEC-218000 of the European Commission's Seventh Framework Programme.

1. E.N. Arkadieva, O.A. Matveev, S.M. Ryvkin, and Yu.V. Rud', Zh. Tekhn. Fiz. **36**, 1146 (1966).
2. E.N. Arkadieva, O.A. Matveev, S.M. Ryvkin, and Yu.V. Rud', Fiz. Tekh. Poluprovodn. **1**, 805 (1967).
3. P. Siffert, B. Rabin, H.Y. Tabatabai, and R. Stuck, Nucl. Instrum. Methods **150**, 31 (1978).
4. J.F. Butler, C.L. Lingren, and F.P. Doty, IEEE Trans. Nucl. Sci. **39**, 605 (1992).
5. A. Burger, K. Chattopadhyay, H. Chen, J.-O. Ndap, X. Ma, S. Trivedi, S.-W. Kutcher, R. Chen, and R.-D. Rosemeier, J. Cryst. Growth **198/199**, 872 (1999).
6. A. Mycielski, A. Burger, M. Sowinska, M. Groza, A. Szadkowski, P. Wojnar, B. Witkowska, W. Kaliszek, and P. Siffert, Phys. Status Solidi C **2**, 1578 (2005).
7. A. Hossain, Y. Cui, A.E. Bolotnikov, G.S. Camarda, G. Yang, D. Kochanowska, M. Witkowska-Baran, A. Mycielski, and R.B. James, J. Electr. Mater. **38**, 1593 (2009).
8. T. Takahashi, K. Hirose, C. Matsumoto, K. Takizawa, R. Ohno, T. Ozaki, K. Mori, and Y. Tomita, Proc. SPIE **3446**, 29 (1998).
9. T. Takahashi, B. Paul, K. Hirose, S. Matsumoto, R. Ohno, T. Ozaki, K. Mori, and Y. Tomita, Nucl. Instrum. Methods A **436**, 111 (1999).
10. http://www.amptek.com/cdte.html.
11. Cs. Szeles, Phys. Status Solidi B **241**, 783 (2004).
12. S.D. Sordo, L. Abbene, E. Caroli, A.M. Mancini, A. Zappettini, and P. Ubertini, Sensors **9**, 3491 (2009).
13. C. Szeles, S.A. Soldner,S. Vydrin, J. Graves, and D.S. Bale. IEEE Trans. Nucl. Sci. **55**, 572 (2008).
14. http://www.amptek.com/pricelist.html
15. L.A. Kosyachenko and O.L. Maslyanchuk, Phys. Status Solidi C **2**, 1194 (2005).
16. L.A. Kosyachenko, V.A. Gnatyuk, T. Aoki, V.M. Sklyarchuk, O.F. Sklyarchuk, and O.L. Maslyanchuk. Appl. Phys. Lett. **94**, 092109 (2009).
17. L.A. Kosyachenko, V.M. Sklyarchuk, O.F. Sklyarchuk, O.L. Maslyanchuk, V.A. Gnatyuk, and T. Aoki, IEEE Trans. Nucl. Sci. **56**, 1827 (2009).
18. L.A. Kosyachenko, C.P. Lambropoulos, T. Aoki, E. Dieguez, M. Fiederle, D. Loukas, O.V. Sklyarchuk, O.L. Maslyanchuk, E.V. Grushko, V.M. Sklyarchuk, J. Crocco, and H. Bensalah, Semicond. Sci. Technol. **27**, 015007 (2012).
19. H. Shiraki, M. Funaki, Y. Ando, A. Tachibana, S. Kominami, and R. Ohno, IEEE Trans. Nucl. Sci. **56**, 1717 (2009).
20. H. Shiraki, M. Funaki, Y. Ando, S. Kominami, K. Amemiya, and R. Ohno, IEEE Trans. Nucl. Sci. **57**, 395 (2010).
21. D. Kanzer, J. Phys. C **6**, 2967 (1973).
22. N. Peyghambarian, S.W. Koch, and A. Msyrowicz, *Introduction to Semiconductor Optics*, (Prentice-Hall, Englewood Cliffs, 1993).
23. T.E. Schlesinger, J.E. Toney, H. Yoon, E.Y. Lee, B.A. Brunett, L. Franks, and R.B. James, Mater. Sci. Eng. **32**, 103 (2001).
24. L.A. Kosyachenko, V.M. Sklyarchuk, O.V. Sklyarchuk, and O.L. Maslyanchuk, Semiconductors **45**, 1247 (2011).
25. B. Segal, M.R. Lorenz, and R.E. Halsted, Phys. Rev. **129**, 2471 (1963).
26. I. Turkevych, R. Grill, J. Franc, E. Belas, P. Hoschl, and P. Moravec, Semicond. Sci. Technol. **17**, 1064 (2002).
27. M. Prokesch and C. Szeles, Phys. Rev. B **75**, 245204 (2007).
28. V. Babentsov, J. Franc, and R.B. James. Appl. Phys. Lett. **94**, 052102 (2009).
29. K. Seeger, *Semiconductor Physics* (Springer, New York, Wien, 1973).
30. M. Hofmann, W. Stadler, P. Chrismann, and B.K. Meyer, Nucl. Instrum. Methods A **380**, 117 (1996).
31. A. Castaldini, A. Cavallini, B. Fraboni, P. Fernandez, and J. Piqueras, J. Appl. Phys. **83**, 2121 (1998).
32. M. Zha, E. Gombia, F. Bissoli, A. Zappettini, and L. Zanotti, Phys. Status Solidi C **3**, 881 (2002).
33. G. Mandel, Phys. Rev. **134**, A1073 (1964).
34. F.F. Morehead and G. Mandel, Phys. Rev. **137**, A924 (1965).
35. M. Fiederle, C. Eiche, M. Salk, R. Schwarz, K.W. Benz, W. Stadler, D.M. Hofmann, and B.K. Meyer, J. Appl. Phys. **84**, 6689 (1998).
36. M. Chu, S. Terterian, D. Ting, C.C. Wang, H.K. Gurgenian, and S. Mesropian, Appl. Phys. Lett. **79**, 2728 (2001).
37. C.-T. Sah, R.N. Noyce, and W. Shockley, Proc. IRE **45**, 1228 (1957).
38. L.A. Kosyachenko, V.P. Makhniy, and I.V. Potykevich, Ukr. J. Phys. **23**, 279 (1978).
39. S.M. Sze and Kwok K. Ng, *Physics of Semiconductor Devices*, (Wiley Interscience, Murray Hill, NJ, 2006).
40. C. Canali, M. Martini, G. Ottaviani, and K.R. Zanio, Phys. Rev. B **4**, 422 (1971).
41. http://www.amptek.com/xrcdtaps.html.
42. C. Matsumoto, T. Takahashi, K. Takizawa, R. Ohno, T. Ozaki, and K. Mori, IEEE Trans. Nucl. Sci. **45**, 428 (1998).
43. P.N. Luke and M. Amman, IEEE Trans. Nucl. Sci. **54**, 834 (2007).

44. M. Lavagna, J.P. Pique, and Y. Marfaing, Solid State Electron. **20**, 235 (1977).
45. http://physics.nist.gov/PhysRefData/XrayMassCoeff.
46. K. Hecht, Z. Phys. **77**, 235 (1932).
47. http://www.acrorad.co.jp/us/cdte.

Received 16.01.13.
Translated from Ukrainian by O.I. Voitenko

О.Л. Маслянчук, Т. Аокі, В.М. Склярчук,
С.В. Мельничук, Л.А. Косяченко, Є.В. Грушко

ВИСОКОЕФЕКТИВНІ ТЕЛУРИД-КАДМІЄВІ ДЕТЕКТОРИ X- і γ-ВИПРОМІНЮВАННЯ

Р е з ю м е

Досліджено електричні характеристики кристалів CdTe, легованих хлором, з питомим опором (3–6)·10^9 Ом·см. Практично власну електропровідність сильно легованого матеріалу пояснено утворенням самокомпенсованих комплексів, виходячи зі статистики носіїв заряду. Знайдено енергію іонізації і ступінь компенсації домішки, відповідальної за напівізолюючий стан CdTe. Інтерпретовано зворотні вольт-амперні характеристики структури Ni/CdTe/Ni з діодом Шотткі як детекторів X/γ-променів, що забезпечують рекордно низькі значення "темнових" струмів ∼5 нА при напрузі 1500 В, площі контакту Шотткі 0,1 $см^2$(300 K). Представлено результати, які засвідчують енергетичну роздільну здатність детектора у спектрі ізотопу ^{137}Cs: 0,42% при прикладеній напрузі 1200 В (300 K). Доведено, що залежність детектуючої ефективності від концентрації нескомпенсованих домішок (дефектів) N, яка визначає ширину області просторового заряду в діоді, описується функцією з максимумом, який для ізотопу ^{137}Cs припадає на $N \approx 2 \cdot 10^{11}$ $см^{-3}$. Із зіставлення спектрів, отриманих при опроміненні детектора з боку контакту Шотткі і омічного контакту, знайдено концентрацію нескомпенсованих домішок у досліджуваних кристалах ($\sim 10^{12}$ $см^{-3}$), яка близька до оптимального значення N.